

RESEARCH LETTER

10.1002/2016GL068583

Key Points:

- Clouds do not have higher buoyancies in a world with fusion than in a world without it
- Preexisting theories for cloud buoyancy do not predict systematically higher buoyancies in a world with ice
- The large reservoir of CAPE in the upper troposphere is not due to the latent heat of fusion

Correspondence to:

J. T. Seeley,
jseeley@berkeley.edu

Citation:

Seeley, J. T., and D. M. Romps (2016), Tropical cloud buoyancy is the same in a world with or without ice, *Geophys. Res. Lett.*, 43, 3572–3579, doi:10.1002/2016GL068583.

Received 7 MAR 2016

Accepted 22 MAR 2016

Accepted article online 27 MAR 2016

Published online 12 APR 2016

Tropical cloud buoyancy is the same in a world with or without ice

Jacob T. Seeley^{1,2} and David M. Romps^{1,2}

¹Department of Earth and Planetary Science, University of California, Berkeley, California, USA, ²Climate and Ecosystem Sciences Division, Lawrence Berkeley National Laboratory, Berkeley, California, USA

Abstract When convective clouds grow above the melting line, where temperatures fall below 0°C, condensed water begins to freeze and water vapor is deposited. These processes release the latent heat of fusion, which warms cloud air, and many previous studies have suggested that this heating from fusion increases cloud buoyancy in the upper troposphere. Here we use numerical simulations of radiative-convective equilibrium with and without ice processes to argue that tropical cloud buoyancy is not systematically higher in a world with fusion than in a world without it. This insensitivity results from the fact that the environmental temperature profile encountered by developing tropical clouds is itself determined by convection. We also offer a simple explanation for the large reservoir of convective available potential energy in the tropical upper troposphere that does not invoke ice.

1. Introduction

One of the many sources of complexity in atmospheric convection is the fact that cloud water exists not just in gas and liquid form but also in the solid phase. There is ample evidence that ice modifies the radiative properties of clouds [Irvine and Pollack, 1968; Sun and Shine, 1995], and such differences between ice and liquid clouds may be relevant to storm morphology [Liu *et al.*, 1997], mesoscale cloud organization [Grabowski, 2003], and high-latitude climate feedbacks [Cronin and Tziperman, 2015; McCoy *et al.*, 2015]. Ice is also crucial to the most widely accepted mechanism for charge separation in thunderstorms [Takahashi, 1978], so it seems likely that a world without ice would be a world without lightning [Williams, 1989].

The role of ice in determining the dynamical properties of clouds, such as their buoyancy and vertical velocity, is less well settled. However, it is commonly argued that ice is a source of buoyancy for convective clouds that grow above the melting line. In response to a debate about convective instability in the tropics raised by Xu and Emanuel [1989], Williams and Renno [1993] pointed out that accounting for ice significantly increases the convective available potential energy (CAPE) of an undiluted parcel. Reflecting on decades of aircraft observations, Zipser [2003] argued for a conceptual picture of tropical convection in which updrafts in the equatorial trough are heavily diluted by entrainment in the lower troposphere, but reinvigorated above the melting line by the release of latent heat of fusion and thereby powered into the upper troposphere. Similarly, Fierro *et al.* [2009] performed updraft trajectory analyses on a simulated oceanic squall line and also concluded that latent heat released by freezing condensates compensates for low-level entrainment. In a more idealized radiative-convective equilibrium (RCE) framework, Romps and Kuang [2010] used a Lagrangian parcel model with and without ice physics to argue that the latent heat of fusion provides kinetic energy that is necessary for diluted parcels to reach the tropopause.

It is natural to conclude from these results that clouds would be less buoyant and have slower updrafts in a world without ice. The purpose of this paper is to show that this is not the case. Here we use cloud-resolving model (CRM) simulations of tropical RCE with and without ice processes to demonstrate that cloud dynamics—whether measured by the typical buoyancy of diluted cloud air, or the vertical velocities of cloud updrafts, or the CAPE of an undiluted parcel—are essentially unaffected by freezing condensates. The reason for the insensitivity to ice is not some coincidental balance between a buoyancy source from the latent heat of fusion and a buoyancy sink from a different ice process such as condensate loading. Instead, the insensitivity results from the fact that the environmental temperature profile encountered by developing clouds is itself determined by convection. This is true in Earth's tropics, where fast gravity waves enforce nearly moist-convective lapse rates even where there is little local convective heating, and it is also true in our

simulations of RCE. Taking account of this coupled relationship between clouds and their environment reconciles our results with the common claim that ice invigorates convective clouds.

In section 2, we describe how ice is “turned off” in the CRM. We present the results of our RCE simulations with and without ice in section 3, and in section 4 we argue that preexisting theories for cloud buoyancy do not predict larger cloud buoyancies in a world with ice. Finally, section 5 gives an explanation for the top heaviness of tropical undiluted parcel buoyancy profiles that does not invoke ice.

2. Ice in the Cloud-Resolving Model

Our simulations of RCE were performed with Das Atmosphärische Modell (DAM) [Romps, 2008]. Microphysics in DAM is treated with the six-class Lin-Lord-Krueger scheme [Lin et al., 1983; Lord et al., 1984; Krueger et al., 1995]. Of the six classes of water in the microphysics scheme, three are ice: nonprecipitating cloud ice, and precipitating snow and graupel.

The effects of these types of ice on the model atmosphere in DAM can be conceptually divided into several categories: (1) the latent heating of phase changes involving solid water (i.e., freezing/melting and deposition/sublimation); (2) the difference in the saturation vapor pressure with respect to ice and with respect to liquid; (3) the different heat capacities of liquid and solid; (4) the different treatment of solid and liquid cloud water by the interactive radiation scheme; (5) the different fall speeds of snow, graupel, and rain; and (6) the effect of ice microphysics on the conversion of nonprecipitating condensates to precipitation. Since the focus of this work is on the connection between buoyancy and the thermodynamics of ice, we design our experiments to prevent effects 4, 5, and 6 from influencing our results. Effect 4 is eliminated by altering the radiation scheme to treat liquid and ice in the same way. Effect 5 is eliminated by using a homogeneous terminal velocity of 10 m/s for all hydrometeors in all simulations. Instead of eliminating effect 6, we ensure that it is present even in the simulations with “no ice,” as described below. These choices allow us to focus on the thermodynamic effects of ice (effects 1–3). We have also checked that our main results are unmodified by these simplified treatments of fall speeds and cloud radiative properties.

In fact, the first three effects of ice listed above are related through the expression for the saturation-specific humidity, q_v^* ; the value of q_v^* differs with respect to ice and liquid solely due to the nonzero latent heat of fusion and the difference between the heat capacity of liquid and solid water (see the Appendix of Romps [2015] for explicit expressions for q_v^*). In particular, the latent heat of fusion in DAM is $L_f = E_{0s} + (c_{vl} - c_{vs})(T - T_{\text{trip}})$, where the constant $E_{0s} = 3.337 \times 10^5$ J/kg is the specific internal energy difference between liquid and solid water at the triple-point temperature $T_{\text{trip}} = 273.16$ K, and the specific heat capacity at constant volume of liquid water is $c_{vl} = 4216$ J/kg/K, which is roughly twice the corresponding quantity for solid water ($c_{vs} = 2106$ J/kg/K). L_f is approximately 13% of the latent heat of condensation, L_c , at the triple point.

In this work, we will refer to simulations and parcel calculations “with ice” and “without ice”: when ice is turned on, E_{0s} and c_{vs} take their physically realistic values as listed above; when ice is turned off, $E_{0s} = 0$ and $c_{vs} = c_{vl}$ so that $L_f = 0$. Although DAM simulations without ice still keep track of the partitioning of condensed water between the liquid and solid categories, the homogenized heat capacities, fall speeds, radiative properties, and the neglect of the latent heat of fusion ensure that the two phases are treated completely identically, so the model’s distinction between them has no physical consequence. In simulations with a meaningful ice phase, DAM allows for nonisothermal mixed phase clouds by assuming that the fraction of liquid cloud condensates is a unique function of temperature, decreasing linearly from 1 at T_{trip} to 0 at 240 K. For consistency with the CRM, we assume the same mixed phase process for our parcel calculations; the method for calculating parcel properties in the present work is identical to that described in detail in section 3c of Romps [2015].

3. RCE Simulations With and Without Ice

The state of radiative-convective equilibrium is a first approximation to Earth’s tropical atmosphere, and many aspects of RCE simulations compare very favorably to tropical observations. Distributions of cloud buoyancy in high-resolution CRMs have been shown to match the results of field campaigns quite well [e.g., Romps and Oktem, 2015, Figure 2], and simulated RCE states reproduce the “C”-shaped relative humidity profiles [Romps, 2014] and trimodal cloud fraction profiles [Dessler et al., 2006] that characterize Earth’s tropics. This makes RCE an excellent tool for testing theories about tropical convection.

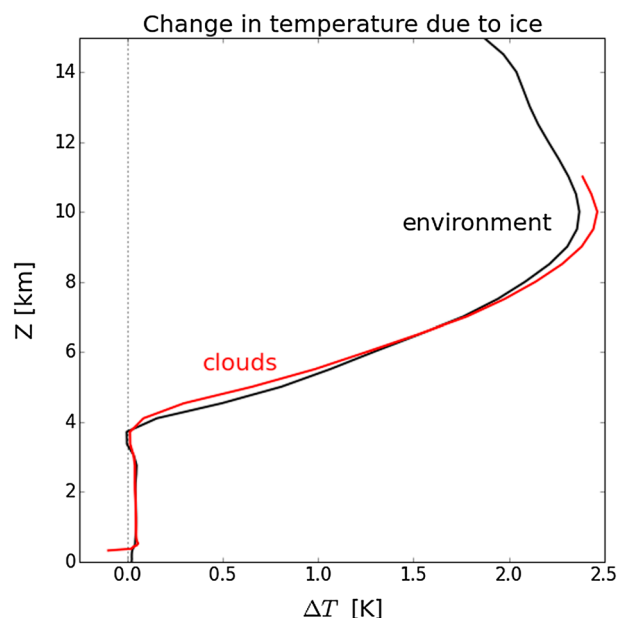


Figure 1. Absolute temperature differences between the simulation with ice and without ice. The environmental (i.e., time mean and domain mean) temperature difference is shown in black, and the cloud updraft temperature difference is shown in red. The cloud temperature is determined by conditionally sampling all grid points with vertical velocity larger than 1 m/s and nonprecipitating condensed water mass fraction larger than 10^{-5} kg/kg, and is plotted only where clouds are positively buoyant in the mean.

We ran two simulations of tropical convection over a fixed sea surface temperature (SST) of 300 K, with interactive radiation and surface fluxes computed via a standard bulk formula; the two simulations differ only by the presence or absence of ice processes, determined by setting the appropriate values for E_{0s} and c_{vs} as described in section 2. Each simulation was initialized from a standard RCE sounding, with random temperature noise of amplitude 0.5 K added to the lowest model level to break the translational symmetry and run to RCE over the course of approximately 50 days on a doubly periodic, 36 km domain with a model top at 40 km and 500 m horizontal resolution. The simulations were then restarted on the same domain but with 200 m grid spacing and run for an additional 25 days; the simulations adjusted to the higher resolution within 10 days, and statistics were collected over the last 15 days of equilibrated convection (during the equilibrated averaging period, the magnitude of the total energy tendency in the model was smaller than 0.3 W/m^2). Horizontal mean and time mean vertical profiles of quantities of interest were recorded, as well as mean profiles within “cloud updrafts.” Cloud updrafts were identified as any grid cell with nonprecipitating condensed water mass fraction greater than 10^{-5} kg/kg and vertical velocity greater than 1 m/s. Our results would be largely unchanged if we had used the data from the simulations with 500 m horizontal resolution.

Figure 1 shows that turning on ice in our simulations increases the mean temperature of cloud updrafts above the melting line by up to nearly 2.5 K (red line). This is a very large change compared to the typical buoyancies of observed and simulated tropical oceanic convective clouds, which are less than 0.5 K when reported as condensate-loaded virtual temperature anomalies [e.g., Lawson and Cooper, 1990; Wei *et al.*, 1998; Sherwood *et al.*, 2013; Romps and Charn, 2015]. However, Figure 1 also shows that the warming of the environmental temperature due to ice (black line) is essentially identical to the cloud warming between the altitudes of 500 m and 11 km, where clouds are positively buoyant in the mean. The fact that the latent heat of fusion released by deposition and freezing increases the temperature of both clouds and their environment—without changing the difference between these temperatures—is one of the key points of this paper.

In Figure 2a, we plot the mean buoyancy of cloud updrafts in the simulations with and without ice. In both simulations cloud buoyancy is between 0.01 and 0.02 m/s^2 (i.e., an effective temperature excess of $\sim 0.25\text{--}0.5$ K) between 1 and 10 km. There is no increase in cloud buoyancy above the melting line (at roughly 4.3 km) in the simulation with ice. In fact, there is a kink in the buoyancy profile toward lower values at this altitude in the simulation with ice. The explanation for this kink is the same as for the kink in buoyancy at the cloud base: in the presence of a vertically continuous radiative cooling rate and a vertically discontinuous static stability

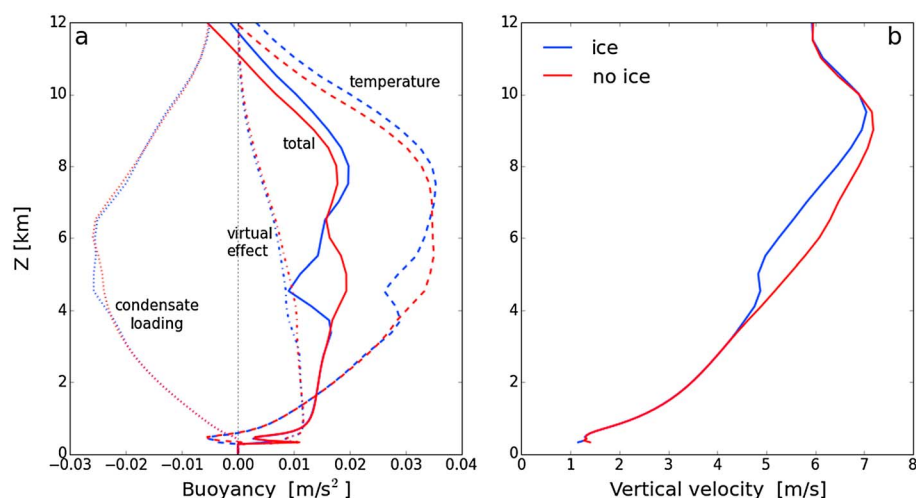


Figure 2. (a) Mean buoyancy of cloud updrafts in the simulation with ice (blue) and without ice (red). Total buoyancy is plotted with solid lines, buoyancy due to temperature differences is plotted with dashed lines, buoyancy due to condensate loading is plotted with dotted lines, and buoyancy due to the virtual effect is plotted with dash-dotted lines (see equation (1) for expressions for these contributions). (b) Mean vertical velocity of cloud updrafts in the two simulations. For both plots, cloud updraft properties are determined by conditionally sampling grid points with thresholds for vertical velocity and condensed water mass fraction (see text).

(discontinuities at the transition from dry adiabat to liquid moist adiabat at the cloud base and from liquid moist adiabat to ice moist adiabat at the melting line), a steady state profile of environmental temperature requires a discontinuity in mass flux, which is generated by a bump in the environment’s potential temperature profile (i.e., a slight capping “inversion”) that weeds out some of the less buoyant updrafts. In the profiles of cloud buoyancy, these bumps in potential temperature manifest as negative excursions of cloud buoyancy.

The relative insensitivity of total buoyancy to ice is not due to a compensation between the effects of ice on different sources of buoyancy. This can be seen by decomposing the buoyancy of moist air into its sources as follows:

$$b \simeq g \left[\frac{\Delta T}{T} + \left(\frac{R_v}{R_d} - 1 \right) \Delta q_v - \Delta q_{\text{con}} \right], \quad (1)$$

where g is the gravitational acceleration, R_v and R_d are the gas constants for water vapor and dry air, and ΔT , Δq_v , and Δq_{con} are the temperature, water vapor, and condensed water anomalies of the cloud relative to the environment, respectively. We decompose the total buoyancy into the temperature, virtual effect, and condensate-loading contributions in Figure 2a to show that each of the individual terms contributing to buoyancy is more or less constant between the two simulations. We also show the mean vertical velocity of cloud updrafts in Figure 2b. Above the melting line, the simulation with ice actually has slightly smaller updraft velocities than the simulation without ice (corresponding to the kink in buoyancy seen in Figure 2a), but these differences are only ~ 0.5 m/s.

Finally, in Figure 3 we show the profiles of undiluted buoyancy for near-surface air parcels lifted through the mean environmental density profiles of the two simulations. Parcels are initialized with the mean thermodynamic properties of the near-surface CRM level of the corresponding simulation, and the parcel buoyancy as a function of height is calculated by assuming conservation of MSE-CAPE, with a definition of MSE that includes the latent heat of the ice phase and the effects of liquid and solid water on the heat capacity of air [Romps, 2015]. To strike a balance between the idealized adiabatic and pseudoadiabatic processes, we assume that half of all condensed water falls out of the parcels immediately upon formation; our results are not overly sensitive to this choice.

There are four buoyancy profiles in Figure 3 because for each of the two mean environmental density profiles generated by our RCE simulations we can lift a near-surface parcel with and without ice processes enabled. (As in the simulations, ice is turned off for the parcel calculations by setting $E_{0s} = 0$ and $c_{vs} = c_{vl}$). The solid lines in Figure 3 show the results when the parcel’s ice thermodynamics match the ice thermodynamics that produced the environmental density profile. In this case, CAPE varies by only 2.5%, increasing by 108 J/kg in

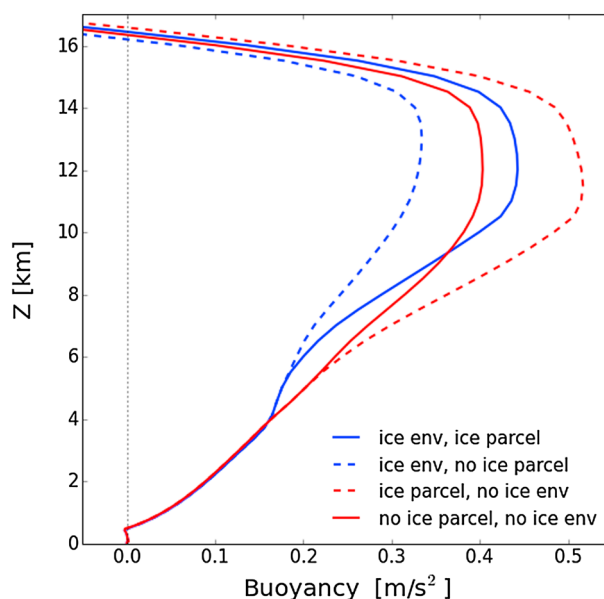


Figure 3. Profiles of buoyancy for undiluted parcels from the RCE simulations. The parcel properties are calculated by lifting air with the mean properties of the near-surface CRM level through the time mean and domain mean density profile, assuming conservation of MSE-CAPE. Half of all condensates are assumed to fall out of the parcel immediately upon formation. Solid lines show results when the parcel and environment ice thermodynamics match and dashed lines show when they are mismatched (see text).

the simulation with ice. If, instead, we calculate CAPE with mismatched thermodynamic assumptions—that is, if we lift a parcel with ice processes enabled through the environment from the simulation in which ice was disabled, or vice versa—the CAPE change is almost an order of magnitude larger (Figure 3, dash-dotted lines). Disabling ice for the parcel that is lifted through the ice environment reduces its CAPE by 850 J/kg, while enabling ice for the parcel that is lifted through the no ice environment increases its CAPE by a similar amount.

4. Theoretical Discussion

It is important to distinguish between two questions that are often conflated: (1) given an environmental temperature profile, does fusion increase the buoyancy of a convecting cloud and (2) does an atmosphere with fusion have larger cloud buoyancies than an atmosphere with no fusion? Question 1 is the one addressed by *Williams and Renno* [1993], *Fierro et al.* [2009], and *Romps and Kuang* [2010]. The answer, which is “yes,” can be seen in Figure 3 by comparing the solid blue and dashed blue curves or by comparing the solid red and dashed red curves: given an environmental temperature profile, a cloud that ascends with fusion has a higher buoyancy than a cloud that ascends without fusion. Question 2 asks whether a world with fusion has higher cloud buoyancies than a world without fusion. The answer, which is “no,” can be seen by comparing the solid blue and solid red curves in Figures 2a and 3: a world with fusion does not have systematically higher cloud buoyancies than a world without fusion.

At present, there is no complete theory for what determines cloud buoyancy in a moist atmosphere. Nevertheless, there are two plausible ideas about cloud buoyancy, and neither of them would predict a significantly larger cloud buoyancy in a world with ice compared to a world without ice. One of those ideas is that actual cloud buoyancy can be described as some fraction of the undiluted cloud buoyancy. The other idea is that the actual cloud buoyancy is dictated by the mismatch in height between the profiles of latent heating and radiative cooling. We will discuss each of these in turn.

The first idea is that cloud buoyancy is some fraction of undiluted cloud buoyancy, and this idea stems from the recent theory for tropical CAPE [*Singh and O’Gorman*, 2013]. In this theory, the atmosphere is approximately neutrally stable to the commonplace moist entraining cloud. Therefore, CAPE is simply the vertical integral of the buoyancy that is given by the temperature difference between an undiluted parcel and a parcel that entrains with the typical entrainment rate. This theory has been validated with a variety of tests in large-eddy simulations [*Singh and O’Gorman*, 2013; *Seeley and Romps*, 2015].

Now, if all clouds had exactly the same entrainment rate and if the atmosphere were exactly neutrally stratified with respect to those clouds, then no cloud would have any buoyancy. In reality, different clouds begin with different entropies (set by the distribution of entropy in the boundary layer) and different clouds experience different amounts of dilution (set by a distribution of entrainment rates in the free troposphere). The mean cloud buoyancy will be set by both of these distributions, leading to a mean cloud buoyancy that is some fraction of the undiluted cloud buoyancy. Assuming the distributions of boundary layer entropy and free-tropospheric entrainment are unaffected in any significant way by the presence or absence of fusion (as is the case in our simulations), the ratio of mean cloud buoyancy to undiluted cloud buoyancy should likewise be independent of the presence or absence of fusion.

Therefore, according to this idea, mean cloud buoyancy should change in proportion to undiluted cloud buoyancy. Or, averaged over the troposphere, cloud buoyancy should change in proportion to CAPE. Recall that CAPE is proportional to the integrated temperature difference between entraining and nonentraining parcel profiles. At a given height, that temperature difference is proportional to the amount of latent heat released up to that height. Therefore, neglecting the effects of lofted condensates (i.e., assuming that both entraining clouds and the undiluted parcel quickly drop their condensed water), the existence of fusion (compared to a world with no fusion) causes a fractional increase in upper tropospheric cloud buoyancy of roughly $(L_f/L_c) \times [q_v^*(\text{melting line})/(q_v^*(\text{cloud base}))]$ (i.e., the fractional increase in latent heat from fusion times the portion of the parcel's water vapor that condenses above the melting line). This predicts an increase in upper tropospheric buoyancy of $\sim 4\%$ due to fusion; the corresponding prediction for the increase in CAPE would be something closer to $\sim 2\%$ since fusion affects buoyancy only in the upper troposphere while CAPE is an integral over the entire troposphere. Therefore, this line of argument predicts that mean cloud buoyancy, averaged over the troposphere, would be only $\sim 2\%$ larger in a world with ice compared to a world without ice.

The second idea is that cloud buoyancies are controlled by the vertical profile of net latent heating minus radiative cooling since cloud buoyancies generate sensible heat fluxes. As pointed out by *Mapes* [2001], there is appreciable radiative cooling in cold layers of the atmosphere where latent heating is constrained to be quite small due to the vanishing of q_v^* ; this cooling must, therefore, be balanced primarily by sensible heat fluxes (i.e., $M c_p \Delta T$, where M is the cloud mass flux and ΔT is the temperature anomaly of the clouds). From this perspective, cloud buoyancy (roughly proportional to ΔT) in the upper troposphere exists because radiative cooling cannot be balanced by local latent heating there. It then follows that a world with ice should have about 10% more upper tropospheric latent heating than a world without ice (since deposition releases about 10% more latent enthalpy than condensation). By this line of argument, a world with ice should have a slightly *smaller* sensible heat flux and, therefore, slightly *smaller* cloud buoyancies.

The magnitude of this effect can be estimated by comparing the need for sensible heat fluxes in our two simulations. Let $LH(z)$ (W/m^2) be the net latent heating from condensation and freezing/deposition, vertically integrated from altitude z to the top of the atmosphere. We can use our simulation output to calculate that turning on fusion increases LH by $\leq 10\%$ between 6 km and the anvil height of 12 km, confirming our simple estimate that there should be about 10% more upper tropospheric latent heating in a world with ice. Therefore, assuming radiative cooling does not change, this increase in latent heating in the simulation with fusion would require a decrease in sensible heat flux, $\Delta SH(z)$, of $(0.1)LH$. Estimating LH as $ML_c q_v^*(1 - RH)$, the fractional decrease in sensible heat flux is

$$\frac{\Delta(SH)}{SH} = \frac{(0.1)ML_c q_v^*(1 - RH)}{(M c_p \Delta T)}. \quad (2)$$

Taking $L_c = 2.5 \times 10^6$ J/kg, $q_v^* \leq 3$ g/kg, $RH \geq 60\%$, $c_p = 1000$ J/kg/K, and $\Delta T \sim 1$ K, we estimate a fractional decrease in sensible heat flux of $\leq 30\%$ in the upper troposphere of the simulation with fusion. Assuming cloud mass flux does not change, this implies a $\leq 30\%$ decrease in the mean temperature anomaly of upper tropospheric clouds, and a corresponding $\sim 10\%$ decrease in the troposphere mean cloud buoyancy, in the simulation with fusion.

In summary, we have two different plausible ideas about cloud buoyancy, and neither predict a significantly larger cloud buoyancy in a world with ice as compared to a world without ice. The idea based on CAPE predicts a change in cloud buoyancy of roughly $+2\%$, while the idea based on the vertical distribution of latent and radiative heating predicts a change in cloud buoyancy of roughly -10% . In the CRM, the existence of fusion changes cloud buoyancy with variable sign and a typical magnitude of ≤ 0.01 K over the troposphere.

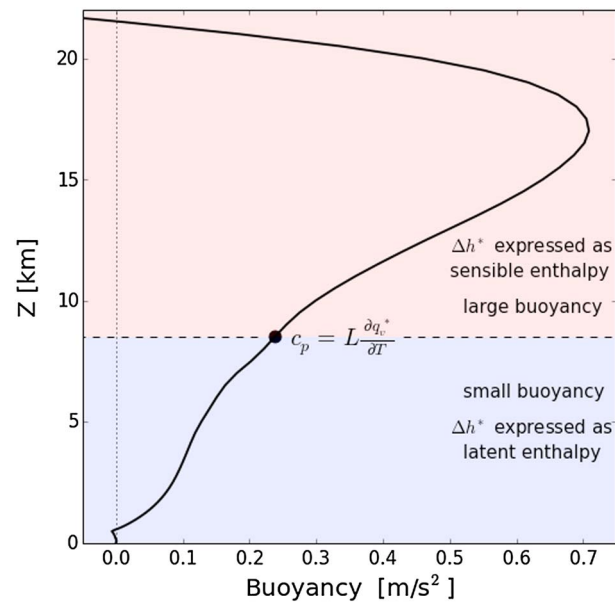


Figure 4. Buoyancy of an adiabatically lifted near-surface parcel from an RCE simulation over an SST of 310 K. The dashed line and black dot mark the level where $c_p = L \frac{\partial q_v^*}{\partial T}$, which serves as an approximate division between the layer of the troposphere where the saturated MSE excess of an undiluted parcel (Δh^*) is primarily expressed as latent enthalpy ($L\Delta q_v^*$), and the layer where Δh^* is primarily expressed as sensible enthalpy ($c_p\Delta T$). Relatively large adiabatic parcel buoyancies are only expected in the sensible enthalpy-dominated regime.

This leads to a troposphere-averaged ice-induced change in cloud buoyancy of -4% , which sits in between the two predictions.

Generally, the claim that cloud buoyancy should be larger above the melting line due to the latent heat of fusion—made by Zipser [2003] and many others—ignores the link between cloud temperatures and environmental temperatures. But, this link is a fundamental property of a convecting atmosphere with fast gravity waves. The release of the latent heat of fusion above the melting line does not increase cloud buoyancy because that latent heat release is not a “surprise” to the environment, but is already imprinted on the environmental temperature by gravity wave adjustment. Therefore, meteorologists on an alternate Earth with no ice phase would find cloud buoyancies and updraft speeds in the upper troposphere that are not significantly different from our own.

5. Why Is Undiluted Buoyancy Largest in the Upper Troposphere?

We have shown that the release of latent heat of fusion above the melting line is not the reason that tropical undiluted parcel buoyancies, such as in our Figure 3 or the observations shown in Figure 5 of Mapes [2001], are largest in the upper troposphere. What, then, is responsible for the “shape of CAPE”?

In fact, the top heaviness of tropical undiluted buoyancy profiles can be explained with concepts borrowed from the theory for CAPE introduced by Singh and O’Gorman [2013], which has also been at the heart of recent progress in our understanding of tropical vertical velocities and relative humidity profiles [Singh and O’Gorman, 2015; Romps, 2014]. As mentioned in section 4, this theory assumes that the temperature profile of the environment in an RCE state is equal to and set by the temperature of an entraining cloud plume; CAPE for an undiluted parcel is then a consequence of the fact that commonplace clouds entrain subsaturated environmental air, thereby setting an environmental temperature that is colder than that of an undiluted parcel.

Seeley and Romps [2015] pointed out that this framework predicts parcel-environment temperature differences to be maximized in the upper troposphere, where the smallness of q_v^* forces the difference in moist static energy between the undiluted parcel and the entraining cloud plume to be expressed as sensible heat ($c_p\Delta T$, where c_p is the heat capacity of dry air) rather than latent enthalpy ($L\Delta q_v$, where L is the latent heat of vaporization). More precisely, if the effect of entrainment is to reduce the moist static energy of the clouds setting the environmental temperature profile by an amount Δh^* , where $h^* = c_pT + Lq_v^* + gz$, then the

temperature difference between an undiluted parcel and the environment at a given height is approximately given by $\Delta h^*/\beta$, where $\beta = (c_p + L \frac{\partial q_v^*}{\partial T})$. In layers of the atmosphere where $L \frac{\partial q_v^*}{\partial T} > c_p$, Δh^* is not predominantly expressed as a parcel-environment temperature difference; this is the case in the lower troposphere for typical conditions in Earth's tropics. It is in the upper troposphere that parcel-environment temperature differences are largest, because there $c_p \gg L \frac{\partial q_v^*}{\partial T}$. (For example profiles of β and Δh^* , see Figure 1 of Seeley and Romps [2015].)

We illustrate this point in Figure 4, where we show the profile of buoyancy for an adiabatically lifted parcel from an RCE simulation that is identical to the no ice simulation with 500 m grid spacing discussed in section 2, except that the SST was set to 310 K instead of 300 K (we use a higher SST simply because it enlarges the features of the buoyancy profile that are our focus). There is clearly a large upper tropospheric peak in undiluted buoyancy in this simulation, despite the lack of ice physics. The black dot on the buoyancy profile marks the altitude where $c_p = L \frac{\partial q_v^*}{\partial T}$, approximately marking the altitude at which the undiluted parcel buoyancy rapidly increases due to the moist-to-dry transition of β discussed above and in Seeley and Romps [2015]. These results suggest that finite and ubiquitous tropical CAPE from top heavy buoyancy profiles is not an accident of the existence of ice but results from simpler two-phase water thermodynamics.

Acknowledgments

This work was supported by the Scientific Discovery through Advanced Computing (SciDAC) program funded by the U.S. Department of Energy Office of Advanced Scientific Computing Research and Office of Biological and Environmental Research under contract DE-AC02-05CH11231. J.T.S. acknowledges support from the National Science Foundation Graduate Research Fellowship under grant DGE1106400. This research used resources of the National Energy Research Scientific Computing Center, a DOE Office of Science User Facility supported by the Office of Science of the U.S. Department of Energy under contract DE-AC02-05CH11231. All simulation outputs used to make the figures in this paper are available from the first author upon request.

References

- Cronin, T. W., and E. Tziperman (2015), Low clouds suppress Arctic air formation and amplify high-latitude continental winter warming, *Proc. Natl. Acad. Sci. U.S.A.*, *112*, 11,490–11,495, doi:10.1073/pnas.1510937112.
- Dessler, A. E., S. P. Palm, and J. D. Spinhirne (2006), Tropical cloud-top height distributions revealed by the Ice, Cloud, and Land Elevation Satellite (ICESat)/Geoscience Laser Altimeter System (GLAS), *J. Geophys. Res.*, *111*, D12215, doi:10.1029/2005JD006705.
- Fierro, A. O., J. Simpson, M. A. LeMone, J. M. Straka, and B. F. Smull (2009), On how hot towers fuel the Hadley cell: An observational and modeling study of line-organized convection in the equatorial trough from TOGA COARE, *J. Atmos. Sci.*, *66*(9), 2730–2746, doi:10.1175/2009JAS3017.1.
- Grabowski, W. W. (2003), Impact of ice microphysics on multiscale organization of tropical convection in two-dimensional cloud-resolving simulations, *Q. J. R. Meteorol. Soc.*, *129*(587), 67–81, doi:10.1256/qj.02.110.
- Irvine, W., and J. Pollack (1968), Infrared optical properties of water and ice spheres, *Icarus*, *360*(4), 324–360, doi:10.1016/0019-1035(68)90083-3.
- Krueger, S. K., Q. Fu, K. N. Liou, and H.-N. S. Chin (1995), Improvements of an ice-phase microphysics parameterization for use in numerical simulations of tropical convection, *J. Appl. Meteorol.*, *34*(1), 281–287.
- Lawson, R. P., and W. A. Cooper (1990), Performance of some airborne thermometers in clouds, *J. Atmos. Oceanic Technol.*, *7*(3), 480–494, doi:10.1175/1520-0426(1990)007<0480:POSATI>2.0.CO;2.
- Lin, Y.-L., R. D. Farley, and H. D. Orville (1983), Bulk parameterization of the snow field in a cloud model, *J. Clim. Appl. Meteorol.*, *22*, 1065–1092.
- Liu, C., M. W. Moncrieff, and E. J. Zipser (1997), Dynamical influence of microphysics in tropical squall lines: A numerical study, *Mon. Weather Rev.*, *125*(9), 2193–2210, doi:10.1175/1520-0493(1997)125<2193:DIOMIT>2.0.CO;2.
- Lord, S. J., H. E. Willoughby, and J. M. Piotrowicz (1984), Role of a parameterized ice-phase microphysics in an axisymmetric, nonhydrostatic tropical cyclone model, *J. Atmos. Sci.*, *41*, 2836–2848, doi:10.1175/1520-0469(1984)041<2836:ROAPIP>2.0.CO;2.
- Mapes, B. (2001), Water's two scale heights: The moist adiabat and the radiative troposphere, *Q. J. R. Meteorol. Soc.*, *127*, 2353–2366.
- McCoy, D. T., D. L. Hartmann, M. D. Zelinka, P. Ceppi, and D. P. Grosvenor (2015), Mixed-phase cloud physics and Southern Ocean cloud feedback in climate models, *J. Geophys. Res. Atmos.*, *120*, 9539–9554, doi:10.1002/2015JD023603.
- Romps, D. M. (2008), The dry-entropy budget of a moist atmosphere, *J. Atmos. Sci.*, *65*(12), 3779–3799, doi:10.1175/2008JAS2679.1.
- Romps, D. M. (2014), An analytical model for tropical relative humidity, *J. Clim.*, *27*(19), 7432–7449, doi:10.1175/JCLI-D-14-00255.1.
- Romps, D. M. (2015), MSE minus CAPE is the true conserved variable for an adiabatically lifted parcel, *J. Atmos. Sci.*, *72*, 3639–3646.
- Romps, D. M., and A. B. Charn (2015), Sticky thermals: Evidence for a dominant balance between buoyancy and drag in cloud updrafts, *J. Atmos. Sci.*, *72*, 2890–2901.
- Romps, D. M., and Z. Kuang (2010), Do undiluted convective plumes exist in the upper tropical troposphere?, *J. Atmos. Sci.*, *67*(2), 468–484, doi:10.1175/2009JAS3184.1.
- Romps, D. M., and R. Oktem (2015), Stereo photogrammetry reveals substantial drag on cloud thermals, *Geophys. Res. Lett.*, *42*, 5051–5057, doi:10.1002/2015GL064009.
- Seeley, J. T., and D. M. Romps (2015), Why does tropical convective available potential energy (CAPE) increase with warming?, *Geophys. Res. Lett.*, *42*, 10,429–10,437, doi:10.1002/2015GL066199.
- Sherwood, S. C., D. Hernández-Deckers, M. Colin, and F. Robinson (2013), Slippery thermals and the cumulus entrainment paradox, *J. Atmos. Sci.*, *70*(8), 2426–2442, doi:10.1175/JAS-D-12-0220.1.
- Singh, M. S., and P. A. O'Gorman (2013), Influence of entrainment on the thermal stratification in simulations of radiative-convective equilibrium, *Geophys. Res. Lett.*, *40*, 4398–4403, doi:10.1002/grl.50796.
- Singh, M. S., and P. A. O'Gorman (2015), Increase in moist-convective updraft velocities with warming in radiative-convective equilibrium, *Q. J. R. Meteorol. Soc.*, *17*, 1–12.
- Sun, Z., and K. P. Shine (1995), Parameterization of ice cloud radiative properties and its application to the potential climatic importance of mixed-phase clouds, *J. Clim.*, *8*(7), 1874–1888, doi:10.1175/1520-0442(1995)008<1874:POICRP>2.0.CO;2.
- Takahashi, T. (1978), Riming electrification as a charge generation mechanism in thunderstorms, *J. Atmos. Sci.*, *35*, 1536–1548.
- Wei, D., A. M. Blyth, and D. J. Raymond (1998), Buoyancy of convective clouds in TOGA COARE, *J. Atmos. Sci.*, *55*(22), 3381–3391, doi:10.1175/1520-0469(1998)055<3381:BOCCIT>2.0.CO;2.
- Williams, E., and N. Renno (1993), An analysis of the conditional instability of the tropical atmosphere, *Mon. Weather Rev.*, *121*, 21–36, doi:10.1175/1520-0493(1993)121<0021:AAOTCI>2.0.CO;2.
- Williams, E. R. (1989), The tripole structure of thunderstorms, *J. Geophys. Res.*, *94*(D11), 13,151–13,167, doi:10.1029/JD094iD11p13151.
- Xu, K.-M., and K. A. Emanuel (1989), Is the tropical atmosphere conditionally unstable?, *Mon. Weather Rev.*, *117*, 1471–1479.
- Zipser, E. J. (2003), Some views on "Hot Towers" after 50 years of tropical field programs and two years of TRMM data, *Meteorol. Monogr.*, *29*, 49–58.